JPEDAV (2005) 26:234-239
DOI: 10.1361/15477030523544
1547-7037/$19.00 ©ASM International

Experimental Investigation and Thermodynamic Calculation of Binary Mg-Mn Phase Equilibria

J. Gröbner, D. Mirkovic, M. Ohno, and R. Schmid-Fetzer

(Submitted January 18, 2005)

The monotectic reaction $L'' = L' + \delta Mn$ in the binary system Mg-Mn was measured at about 1200 °C using differential thermal analysis. This was possible by sealing the samples in arc welded Ta capsules, thus solving the problem of high vapor pressure of Mg at such high temperature and also suppressing any reaction of Mg with the environment. Problems associated with the reaction of Mn with the Ta crucible are discussed in detail. In addition, a thermodynamic assessment and calculation of the entire Mg-Mn phase diagram was performed, incorporating published experimental data on the Mn solubility in the Mg-rich corner.

1. Introduction

Manganese is an important alloying element of magnesium alloys because it eliminates the Fe impurities responsible for poor corrosion properties of Mg alloys. The improvement of corrosion resistance originates from two effects. First, Mn addition decreases the solubility of Fe in Mg drastically and therefore leads to the precipitation of Fe, which settles down in the Mg melt. Moreover, Mn forms a protecting layer during oxidation of Mg. For these reasons, Mn is added to commercial Mg alloys in small amounts.

Experimental data were found only for the Mg-rich corner (0-3.7 at.% Mn) of the Mg-Mn phase diagram. The liquidus temperatures in the range of primary (Mg) were determinated by thermal analysis [1943Gro, 1950Sch, 1957Pet], an ascending liquidus temperature with increasing Mn was reported, a peritectic reaction at about 651 or 653 °C was assumed. Liquidus temperatures for alloys of more than 0.9 at.% Mn were reported by [1943Gro, 1944Bee, 1944Gru, 1945Tin, 1948Sie, 1950Sch, 1957Pet, 1958Chu]. Due to experimental problems, no thermal analytic results are available in this range. All liquidus compositions were obtained by dip sampling. This technique led to several sources of error when the equilibrium was not reached or the solid Mn particles were not completely separated from the analyzed liquid. Therefore Mn contents higher than the equilibrium composition are likely to be measured. Solid solubilities of Mn in (Mg) were determined by [1931Sch, 1943Gro, 1957Pet, 1964Dri] using x-ray analysis. The solubility limit of Mn in (Mg) was reported at 0.99 at.% Mn [1964Dri] and 1.03 at.% Mn [1957Pet]. [1959Dri] found almost no solubility of Mg in Mn.

A summary of all experimental investigations in the Mg-Mn system is given by [1988Nay]. The assessed phase diagram by [1988Nay, 1990Mas] is mainly based on thermal analysis, microscopic observation and hardness measurements of [1957Pet] and resistometric measurements of [1964Dri]. As mentioned above, however, the phase equilibria in Mn-rich and high temperature region have not been studied and are given only qualitatively by a thermodynamic calculation [1998Tib]. In particular, the temperature of the monotectic reaction, $L' = L'' + \delta Mn$, on the Mn-rich side has not been measured before. Considering the similarity to the Li-Mn, Ca-Mn, Sr-Mn, and Ba-Mn binary systems, a miscibility gap has been supposed to exist in the Mg-Mn system. In the current study, we attempt to determine the monotectic reaction temperature on the Mn-rich part by means of a thermoanalytic method and then we present the thermodynamic assessment of the entire Mg-Mn system based on the present experimental results as well as the published Mg-rich experimental data.

2. Experimental Investigation

Four samples (Table 1) were weighed from the elements and sealed into tantalum capsules. The following starting materials were used: Mn chips (99.97 wt.%) and Mg pieces (99.98 wt.%) with both purities referred to the metal basis, not counting the nonmetals as provided by Alfa, Karlsruhe, Germany. Due to high oxygen affinity and vapor pressure of investigated alloys, a special adaptation of the differential thermal analysis (DTA) equipment using sealed Ta crucibles was indispensable for generation of reproducible and reliable data. The Ta-crucibles were produced in our laboratory using a Ta tube with 10 mm outer diameter and 0.4 mm wall thickness and a Ta sheet for the crucible lid and bottom with 0.25 mm thickness of purity, both 99.9 wt.% (metal basis; Plansee GmbH, Reutte, Austria). Each tantalum crucible was filled up to half of the volume with the sample material and sealed, by welding, under argon with 1.5 bar total pressure. Figure 1 shows a cross section of an empty Ta crucible, sealed by electric arc welding. All samples were measured with DTA using a Netzsch DTA 404S apparatus (NETZSCH Gerätebau GmbH, Selb, Germany). High-purity γAl_2O_3 powder was used as the reference material. Prior to measurements, a standard tempera-

J. Gröbner, D. Mirkovic, M. Ohno, and **R. Schmid-Fetzer,** Clausthal University of Technology, Institute of Metallurgy, Robert-Koch-Str. 42D-38678 Clausthal-Zellerfeld, Germany. Contact e-mail: schmid-fetzer@tu-clausthal.de.

Table 1 Experimental DTA results and their interpretation

Sample composition, at.%	Thermal signal °C					
	1st cycle		2nd cycle		Assessed experimental temperature	Interpretation
	Heating(a)(b)	Cooling(a)(c)	Heating(a)(b)	Cooling(a)(c)		
Pure Mg	647 s(d)	650 s	647 s	650 s	650	Liquid = (Mg)
$Mg_{50}Mn_{50}$	646 s	653 s	…	…	649	L′ + αMn = (Mg)
	1125 w(e)	1114 w	1124 w	not detected	1120	(f)
	1196 s	1198 s	1194 w	not detected	1197	L″ = L′ + δMn
	1203 w	1203 w	1201 s	not detected	1203	(f)
$Mg_{20}Mn_{80}$	646 s	647 s	644 s	644 s	646	L′ + αMn = (Mg)
	731 s	not detected	not detected	not detected	731	αMn = βMn, (L′)
	1093 w	1097 w	not detected	not detected	1095	βMn = γMn, (L′)
	1108 w	not certain(h)	1100 w	not detected	1108	(f)
	1135 w	not certain	not detected	not detected	1135	γMn = δMn, (L′)
	1199 s	1198 s	1199 w	not detected	1198	L″ = L′ + δMn
	1203 w	1199 w	not detected	not detected	1201	(f)
$Mg_{10}Mn_{90}$	644 s	645 s	642 s	644 s	644	L′ + αMn = (Mg)
	731 s	not detected	not detected	not detected	731	αMn = βMn, (L′)
	1087 w	1078 w	not detected	not detected	1083	βMn = γMn, (L′)
	1104 w	1096 w	1109 w	not detected	1100	(f)
	not certain	1108 w	not detected	not detected	not certain	(f)
	1137 w	not certain	1127 w	not detected	1137	γMn = δMn, (L′)
	1198 s	1196 s	1199 w	not detected	1197	L″ = L′ + δMn
	1204 w	1197 w	not detected	not detected	1200	(f)
Pure Mn	734 s	not detected	…	…	734	αMn = βMn
	1078 s	not detected	…	…	1078	βMn = γMn
	1138 s	not detected	…	…	1138	γMn = δMn
	1241 s	not detected	…	…	1241	δMn = Liquid

(a) Heating and cooling rates 5K/min; (b) Onset for invariant reactions, peak maximum otherwise; (c) Onset; (d) s, strong and clear signal; (e) w, weak and diffuse signal; (f) Additional or shifted signal, probably caused by reaction with Ta-crucible.

Fig. 1 Cross section of an empty Ta crucible demonstrates the smoothly welded bottom and lid. The DTA thermocouple tip will touch the concave bottom part which is only 0.25 mm thick

ture calibration was performed using the melting point of high-purity Ag, Al, Cu, In, Mg, Pb, and Sb elements. The measurements were performed at 5×10^{-3} mbar static vacuum to protect the outer surface of the Ta crucible in oxidation and to reduce heat exchange in the gas inside the chamber. The overall uncertainty of the DTA measurements was estimated to ±3 K. The DTA measuring program consists of two cycles of 600-1250-600 °C at a heating/cooling rate of 5 K/min with 30 min holding time between the ramps. It is noted that the capsules survived an internal pressure of 10.9 bar, exerted by 7.7 bar of heating the inert argon plus maximum 3.2 bar from the vapor pressure of magnesium.

For all samples except the pure Mn, an additional second cycle of 1000-1250-1000 °C was performed. The reason for skipping the second cycle for the pure Mn sample was to prevent excessive crucible reactions that may lead to a perforation of the Ta crucible and possible damage of DTA equipment. An additional third cycle was performed for the sample Mg10Mn90. After the thermal analysis, the microstructure and the phase equilibra of the samples were examined by scanning electron microscopy with energy dispersive x-ray microanalysis (SEM/EDS). The samples were ground and polished down to 1 μm diamond under alcohol to avoid reaction with water. Etching was not necessary.

3. Experimental Results

Analysis of the DTA curves showed an interesting feature: only the first cycle showed clear and strong signals. Except for the strong thermal signal at a temperature slightly below 650 °C, the heating run of the second cycle showed only weak signals. The same signal was observed during the cooling run of the second cycle but no other signals at all. This trend was even more pronounced with increasing Mn content of the sample. For the pure Mn, no signal was observed after the first formation of melt in the crucible. This effect is explained by reaction of manganese with the tantalum crucible. In the first heating run, the signals of the invariant reactions were clearly detected (Table 1). The sample with pure Mn confirmed the temperatures of the allotropic transformations at 706, 1086, and 1135 °C, which is close to the accepted unary data, 707, 1087, and 1138 °C, respectively. In the binary samples $Mg_{50}Mn_{50}$, $Mg_{20}Mn_{80}$, and $Mg_{10}Mn_{90}$ two invariant reactions were observed: The eutectic reaction L + αMn = (Mg) at just below 650 °C and the monotectic reaction L″ = L′ + δMn at about 1200 °C. After the formation of liquid in the crucible, a reaction with the Ta crucible was observed, and Mn was consumed in the phase $TaMn_2$. This phase forms a layer on the walls of the Ta crucibles, as shown in Fig. 2, taken after three instead of only two heating cycles. The same figure shows a deformation of the Ta crucible due to high internal pressure (10.9 bar at 1250 °C).

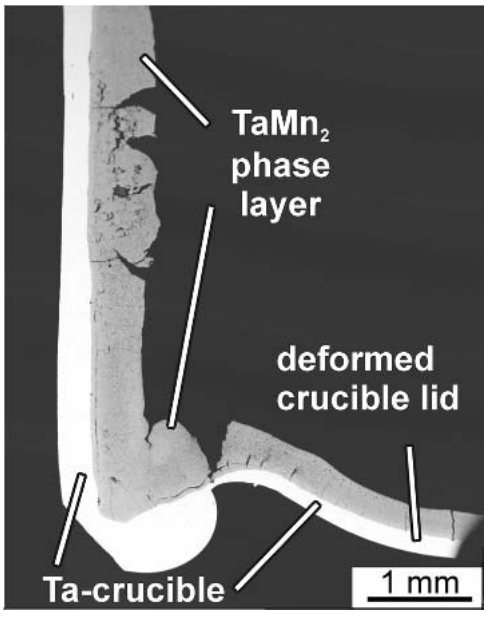

Fig. 2 Secondary electron image of the $Mg_{10}Mn_{90}$ sample showing bottom region of the cross sectioned Ta crucible after three 600-1250-600 °C DTA cycles with 5 K/min scanning rate. The whole Mn is consumed to form $TaMn_2$ phase. The $TaMn_2$ phase forms a layer on the walls of the Ta crucible. The deformation of the crucible bottom due to high internal pressure at higher temperatures is also visible.

4. Thermodynamic Assessment

As a starting point, the thermodynamic data set from the COST database [1998Tib] was used. The molar Gibbs energies for solution phases, liquid, hexagonal close-packed (hcp), face-centered-cubic (fcc) (γMn), body-centered-cubic (bcc) (δMn), complex body-centered-cubic (cbcc) (αMn), and cubic (cub) (βMn), are expressed by the following equation:

$$G^{0,\phi} = x_{Mg} \cdot G^{0,\phi}_{Mg} + x_{Mn} \cdot G^{0,\phi}_{Mn} + RT \cdot (x_{Mg} \ln x_{Mg} + x_{Mn} \ln x_{Mn}) + x_{Mg} \cdot x_{Mn} \cdot \sum_{v=0} L^{v,\phi}_{Mg \cdot Mn} \cdot (x_{Mg} - x_{Mn})^v \quad \text{(Eq 1)}$$

where R is the gas constant; x_{Mg} and x_{Mn} are the molar fractions of Mg and Mn, respectively; $G_i^{0,\phi}$ is the Gibbs energy function for the pure element i in the ϕ phase [1991Din]; and $L^{v,\phi}_{Mg,Mn}$ is the Redlich-Kister parameter.

The interaction parameter of the liquid phase, $L^{v,liquid}_{Mg,Mn}$, was optimized on the basis of the monotectic reaction temperature measured in the current study and the experimental data of [1957Pet]. The thermodynamic description of hcp phases was also improved in the present optimization based on the solubility of Mn in (Mg) measured by [1964Dri]. The parameter ensuring negligible solubility of Mg in the (Mn) solid phases was increased to the value of 85 kJ/mol. Using the previous value of 70 kJ/mol, we detected an artificial stabilization of the δMn (bcc) phase at low temperature in the calculated ternary liquidus surface of the Al-Mg-Mn system. The optimized parameters are listed in Table 2.

The software "Pandat" [2000Pan, 2001Che] was used for the calculations in this work. The resulting calculated phase diagram with the experimental DTA signals is shown in Fig. 3 and the enlargement of the Mg-rich side with the reported experimental data is demonstrated in Fig. 4. The data of [1957Pet] and [1964Dri], highlighted by solid symbols in Fig. 4 are used for optimization since they appear more reliable and they are in agreement with [1944Bee], [1944Gru], and [1950Sch]. One can readily see the overall agreement between the calculated and experimental results. The monotectic reaction temperature for L″ ↔ L′ + δMn is calculated to be 1198 °C, which coincides well with our experimental results, 1200 °C. Furthermore, it is seen that the present calculation reproduces the liquidus temperature of [1957Pet] and the solubility of Mn of [1964Dri] at Mg-rich part (Fig. 4) with quite a high accuracy.

5. Discussion

To the best of our knowledge, the solid solubility of Mg in (Mn) is negligible. Therefore, the solid state transformations of pure Mn at 707, 1087, and 1138 °C must be expected to produce degenerate invariant reactions in the binary Mg-Mn, each at the same temperature. In addition, we have two more truly binary invariant equilibria: L′ + αMn + (Mg) near the melting point of Mg, and L″ + L′ + δMn near the melting point of Mn. All other thermal signals

must be attributed to side effects mainly from the crucible reaction.

The first equilibrium is given by the thermodynamic assessment as a peritectic reaction L′ + αMn = (Mg) at 651 °C based on the Mn solubility data in solid and liquid magnesium (Fig. 4). These data, especially the accepted values of [1957Pet] and [1964Dri], are supporting evidence for a peritectic reaction at a temperature only 1 °C above the melting point of Mg. Compared with these solubility data, the present DTA data are considered to be less important. They show the reaction at a similar temperature, but the trend from 644 to 649 °C with increasing Mg content is impossible in equilibrium. These DTA data where thus not used. The calculated value of 651 °C is well within the error bar of the DTA measurement (± 3 K), at least for the Mg-rich sample.

For the second equilibrium only a monotectic reaction, L″ = L′ + δMn, is possible. The key result of our experimental study is to indicate a temperature for this monotectic, which was not known at all. This requires close scrutiny of the DTA data and separation of any side reactions that may be due to the reaction of Mn with the Ta-crucible or other artifacts, notation as indicated by (f) in Table 1.

As long as the Mn is entirely solid in the sample of pure Mn, all the transitions can be clearly observed, even though the temperatures are somewhat below the accepted unary data. This also applies to the incipient melting observed at 1241 °C. However, after this first melting, all the manganese must have reacted completely to form the stable compound $TaMn_2$ (melting point > 1670 °C [1990Mas]) since on cooling, no solidification signal or other signal could be detected. It is concluded that only the liquefied Mn reacts quickly enough with the crucible. The lower temperature measured, 1241 °C instead of the accepted 1246 °C, may be explained by the fact that only the much lower Mg melting point was used for calibration.

The three binary samples could all produce Mn dissolved in liquid magnesium (i.e., with a chemical activity a_{Mn} = 1), and thus some crucible reaction is expected even at lower temperature and, indeed, observed as those side effect

Table 2 Assessed binary parameters

Phase	Parameter	Value in J/mol
Liquid	$L^{0,liquid}_{Mg,Mn}$	25,922.4 + 9.0357T
	$L^{1,liquid}_{Mg,Mn}$	−3470.8
δMn	$L^{0,bcc}_{Mg,Mn}$	85,000
γMn	$L^{0,fcc}_{Mg,Mn}$	85,000
βMn	$L^{0,cbcc}_{Mg,Mn}$	85,000
αMn	$L^{0,cub}_{Mg,Mn}$	85,000
(Mg)	$L^{0,hcp}_{Mg,Mn}$	37,148.1 − 1.8103T

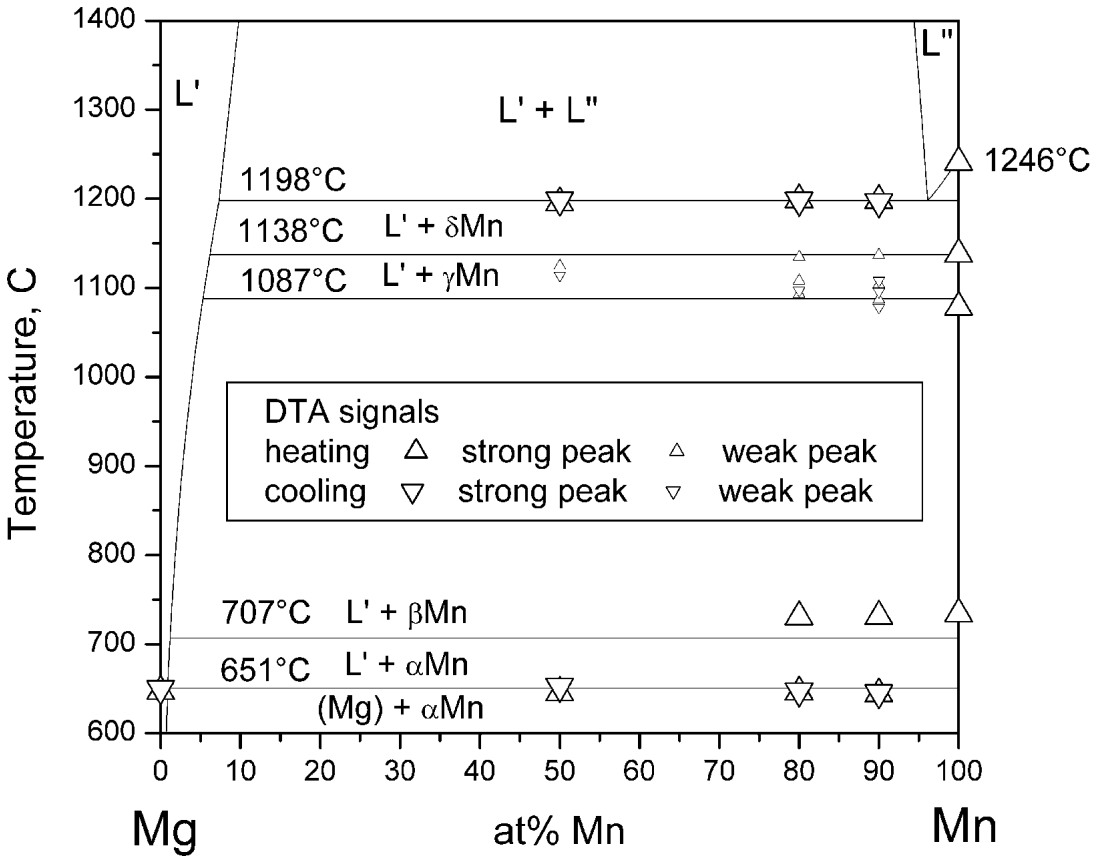

Fig. 3 Calculated Mg-Mn phase diagram compared with our DTA data

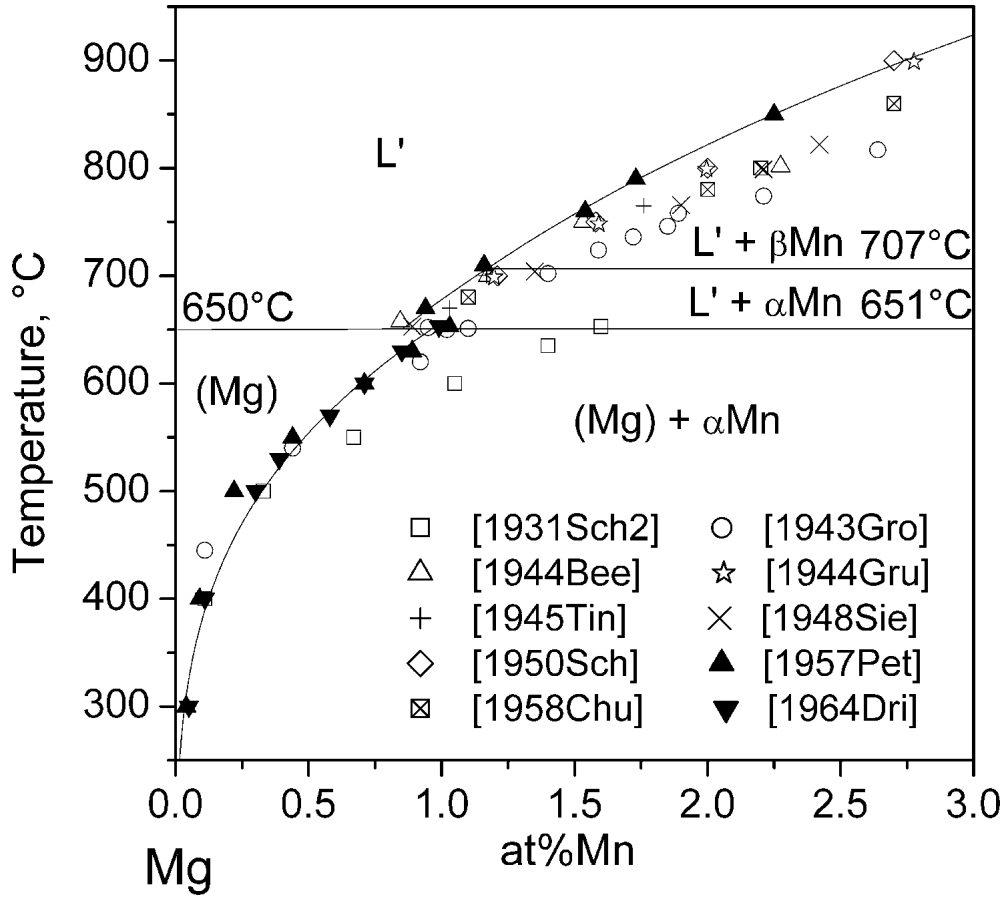

Fig. 4 Calculated Mg-Mn phase diagram in Mg-rich corner compared with experimental data. Solid symbols are accepted for optimization.

signals designated by # in Table 1 that cannot be assigned to any binary Mg-Mn reaction. With this in mind, there is only one signal that could be clearly assigned to the monotectic reaction, the one consistently observed in all three binary samples on heating and cooling in the first cycle at 1198 or 1197 °C at 50 at.% Mn. The second signal at a slightly higher temperature cannot be assigned to the start of the monotectic but may be due to an enhanced crucible reaction since above the monotectic the entire manganese became liquid. The enhanced kinetics of the side reaction also explains the less-clear signals in the first cooling and second heating cycle and especially the missing signals after the second complete melting in the monotectic.

Based on that, we have 1198 °C for the monotectic reaction or 1203 °C if we want to make a correction for the 5 K shifted measurement of the melting point of pure Mn, 1241 °C instead of the accepted 1246 °C [1991Din]. Technically speaking, this is the lower limit of the truly binary $L'' = L' + \delta Mn$ since any dissolved tantalum in the melt would have reduced that temperature as may be estimated from the binary Ta-Mn phase diagram [1990Mas]. However, we do not know how much Ta was actually dissolved; we know only that after the second cycle, all the Mn in the sample had reacted to form $TaMn_2$ as shown in Fig. 2; this is obvious from the DTA data of the second cooling cycle. In spite of this uncertainty, the first experimental value of the monotectic at about 1200 °C was a valuable aid for the thermodynamic calculation that gives this invariant at 1198 °C.

It should be stressed that the DTA measurements without sealing in a crucible are not at all successful due to the high vapor pressure of Mg. Furthermore, different materials for the crucible are not easily used since the sophisticated technique for preparation and sealing of the crucible and fitting to the DTA sensor has to be adapted. An alternative material for the crucible like Mo reacts even faster with Mn due to the large solubility of Mn in Mo. Hence, the present technique using the Ta crucible was the best compromise for determination of the monotectic temperature in this system. It should be emphasized that the accuracy of the thermodynamic calculation in the Mg-rich corner shown in Fig. 4 is not compromised by these difficulties.

Acknowledgment

This study was supported by the German Research Foundation (DFG) in the Priority Program DFG-SPP 1168: InnoMagTe under Grant No. Schm 588/27.

References

1931Sch: E. Schmid and G. Siebel, Determination of Solid Solubility of Mn in Mg by X-Ray Analysis, *Metallwirtschaft,* Vol 10 (No. 49), 1931, p 923-925 (in German)

1943Gro: J.D. Grogan and J.L. Haughton, Alloys of Magnesium. Part XIV. The Constitution of the Magnesium Rich Alloys of Magnesium and Manganese, *J. Inst. Met.,* Vol 69, 1943, p 241-248

1944Bee: A. Beerwald, On the Solubility of Iron and Manganese in Magnesium and Magnesium-Aluminum Alloys, *Metallwissenschaft,* Vol 23, 1944, p 404-407 (in German)

1944Gru: G. Grube, Magnesium-Manganese Phase Diagram, 1944, quoted in [1944Bee]

1945Tin: N. Tiner, The Solubility of Manganese in Liquid Magnesium, *Trans. Met. Soc. AIME,* Vol 161, 1945, p 351-359

1948Sie: G. Siebel, On the Solubility of Iron, Manganese and Zirconium in Magnesium and Magnesium Alloys, *Z. Metallkd.,* Vol 39, 1948, p 22-27 (in German)

1950Sch: A. Schneider and H. Stobbe-Scholder, The Structure and Technical Preparation of Corrosion-Resistant Magnesium-Manganese Alloys, *Metall*., Vol 4 (No. 9-10), 1950, p 178-183

1957Pet: D.A. Petrov, M.S. Mrigalovskaya, I.A. Strelnikova, and E.M. Komova, The Constitution Diagram for the Magnesium-Manganese System, *Trans. Inst. Met. A.A. Baikova, Akad. Nauk SSSR,* 1958, *1,* p 142-143 (in Russian)

1958Chu: M.V. Chukhov, On the Solubility of Mn in Liquid Mg, *Legkie Splaavy, Akad. Nauk SSSR, Inst. Met. A.A. Baikova,* 1958, *1,* p 302-305 (in Russian)

1959Dri: M.E. Drits, Z.A. Sviderskaya, and L.L. Rokhlin, The Nature of the Manganese Phase of Certain Magnesium alloys, *Metalloved. Term. Obrad. Met,* Vol 10, 1959, p 33-37 (in Russian)

1964Dri: M.E. Drits, Z.A. Sviderskaya, and L.L. Rokhlin, Solid Solubility of Mn in Mg, *Izv. Nauka, Moscow,* 1964, p 272-278 (in Russian)

1988Nay: A.A. Nayeb-Hashemi and J.B. Clark, Mg-Mn (Magnesium-Manganese), in *Phase Diagrams of Binary Magnesium Alloys,* edited by A.A. Nayeb-Hashemi and J.B. Clark, ASM International, Materials Park, OH, 1988, p 199-203

1990Mas: T.B. Massalski, P.R. Subramanian, H. Okamoto, and L. Kacprzak, *Binary Alloy Phase Diagrams,* 2nd ed., ASM International, Materials Park, OH, Vol 3, 1990.

1991Din: A.T. Dinsdale, Thermochemical Data of the Elements, *Calphad,* Vol 15, 1991, p 317-425

1998Tib: J. Tibballs, System Mg-Mn, in *COST507 - Thermochemical Database for Light Metal Alloys,* edited by I. Ansara, A.T. Dinsdale, and M.H. Rand, European Commission EUR 18499 EN, 1998, p 215-217

2000Pan: Pandat, Phase Diagram Calculation Engine for Multicomponent Systems, CompuTherm LLC, Madison, WI, 2000

2001Che: S-L. Chen, S. Daniel, F. Zhang, Y.A. Chang, W.A. Oates, and R. Schmid-Fetzer, On the Calculation of Multicomponent Stable Phase Diagrams, *J. Phase Equilibria,* Vol 22 (No. 4), 2001, p 373-378